Characteristics and prediction of sound level in extra-large spaces

Chao Wang[a], Hui Ma[a], Yue Wu[b], Jian Kang[*b,c]

[a]School of Architecture, Tianjin University, Tianjin 300072 China
[b]School of Architecture, Harbin Institute of Technology, Harbin 150001 China
[c]School of Architecture, University of Sheffield, Sheffield S10 2TN UK

Abstract

This paper aims to examine sound fields in extra-large spaces, which are defined in this paper as spaces used by people, with a volume approximately larger than 125000 m^3 and absorption coefficient less than 0.7. In such spaces inhomogeneous reverberant energy caused by uneven early reflections with increasing volume has a significant effect on sound fields. Measurements were conducted in four spaces to examine the attenuation of the total and reverberant energy with increasing source-receiver distance, which was then validated by the simulations with image-source method. Results show that the reasons for the total energy's exponential decrease are not only the direct sound, but also the reverberant energy. The prediction difference of total sound pressure level (SPL) between classical formula and the image-source method increases with the volume and decreases with the surface absorption, based on which a critical line separating extra-large spaces from large ones is proposed. Moreover, a newly modified model based on the importance of first reflection from floor is proposed, showing more advantages of sound level prediction in extra-large spaces.

Keywords: Extra-large space; Sound field; Sound pressure level; Prediction

1   Introduction

Many large buildings are being built worldwide to accommodate more and more complicated functions. In those buildings, the sound field plays an important role in the design of acoustic performance and electronic evacuation systems [1]. With the increase of volume, the spatial distribution difference of reverberant energy, which is very important for the characteristics and prediction of sound level in a space, should become more significant but further details about the phenomenon and theory are also needed.

Evidence of this spatial distribution difference was found in various cases. After a series of measurements in performance spaces, with volumes varied from 2900 to 86650 m^3, reverberant energy decreasing with the source-receiver distance was proposed by Barron based on the image-source method in rectangular rooms [2]. And many other investigations

---

*j.kang@sheffield.ac.uk, j.kang@hit.edu.cn

in concert halls were also validated this difference[3, 4]. The same phenomenon was also found in four Japanese churches, with volumes varied from 1000 to 12600 m^3 [5] and twelve Mudejar-Gothic churches in the south of Spain, with volumes varied from 3947 to 10708 m^3 [6]. In St Pauls Cathedral in London, with a volume of 152000 m^3, variations in sound pressure level (SPL) with distance and the contours of equal SPL for $1000Hz$ octave band also suggest some interesting spatial variations although further analysis has not been conducted [7].

Numerous factors have been used to account for inhomogeneous spatial distribution of the reverberant energy. At each reflection of sound wave, different acoustic characteristics of surfaces, such as absorption and scattering [8, 9], affect sound field to varying degrees. Room shapes, which can be categorised by the ratio of three dimensions [10], such as flat space [11, 12] and long space [13, 14, 15], also has a significant influence on the sound field. In some spaces with small subspaces, coupled-space effect was also considered [16]. Other factors which also need to be considered include air absorption and specular early reflections [16, 17, 18].

While large in acoustics mainly means that low-frequency resonance could be paid less attention for the sound field in a room [19], with the continuously increasing volume, early reflections in extra-large space show more significance as a factor and its influence on the sound field has not been studied systematically. The aim of this current paper is therefore to explore the sound energy distribution and its prediction method in extra-large spaces. Measurements in four cases and computer simulation have been used to explore the characteristics of reverberant energy in extra-large spaces and a new modified model has also been proposed.

2   Method

2.1   On-site measurements

On-site measurements were carried out in four cases, with volumes varied from 7000 to 190000 m^3, representing ordinary to large space respectively, as shown in Fig. 1 and Table 1. The shape and acoustic performance of surfaces in four cases are different but all of them are centralized. Other information is shown in Fig. 2, and the RT in this Table 1 is the average reverberation time of three octave bands (500 Hz, 1 kHz and 2 kHz).

Table 1: Geometry and information of four cases

Case	Name	Volume (m^3)	Seats	RT (s)	Receiver points	Background noise (dBA)	Temperature ($°C$)	Humidity (%)
1	Dangxiao auditorium	7200	688	1.1	21	31	30	59
2	HIT indoor stadium	11400	3000	3.9	22	20	20	50
3	TJU indoor stadium	59000	4000	2.2	17	25	19	28
4	Guian Circus Show	190000	\	3.0	10	30	23	70

The SPL values were measured using an omni-directional source with a pink noise signal and calibrated sound level meters. The source points were arranged at the usual performance point or near the central point of the floor at a height of 1.5 m. The receiver height was 1.2 m. Each point was measured three times to obtain the average value. ISO-3382 standard was followed in the equipment selection and measurement process. For the sake of brevity, only the average of three octave bands (500 Hz, 1 kHz and 2 kHz) is presented in this paper. The SPL at all points were more than 15 dB above the background noise in the four cases.
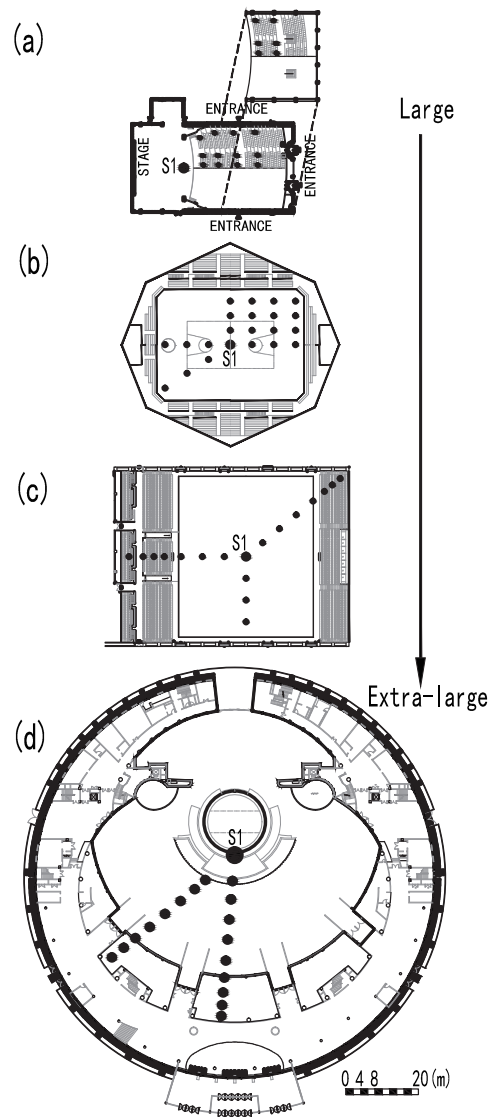
Figure 1: Plans of the four measured spaces with the same scale: (a) Dangxiao auditorium, (b) HIT indoor stadium, (c) TJU indoor stadium, and (d) Guian Circus Show. The source points are labelled S1, receiver positions are shown as black dots.
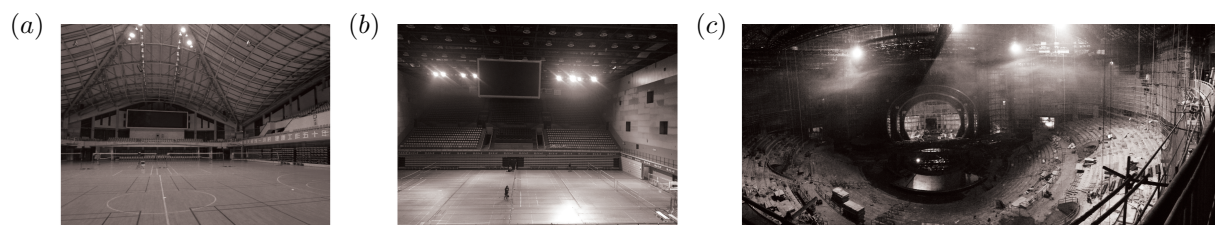

Figure 2: Photograph of three cases: (a) photo of HIT indoor stadium, (b) photo of TJU indoor stadium, and (c) photo of Guian Circus Show. (Only photographs of three larger cases were presented because Dangxiao auditorium's type is so common that general understanding can be obtained from the plan.)

2.2 Computer simulation

Because of the difference in typology, shape, volume, acoustic surface performance, etc., it is difficult to obtain an accurate rule of energy distribution from measurements in different spaces. To control other variables and explore the influence of volume as single factor on sound field, sound energy variation in large spaces have been studied by using computer simulation in a series of hypothetical cubic spaces at different volumes and surface absorptions. An image-source method[20] for cubic spaces has been developed because of its easy-implement algorithm and accuracy of reflection sequence [11, 21]. A great advantage of the image-source model in the current paper is that the calculation accuracy and computational difficulty have no relation to the volume.

The above method has been achieved by using python language to avoid modification algorithms for optimization in some commercial software packages developed for ordinary spaces. By using multi-processing method and customizable pre-processing, the new program shows more flexibility and total efficiency than commercial software packages. In addition, low-frequency resonance, diffraction and edge effect which are less of a concern in extra-large spaces, are not considered. The diffusion effect is also ignored for the sake of convenience.

A total of 20 cubic models were selected, with side length varied from 10 to 500 m (namely, 10, 20, 30, 40, 50, 60, 70, 80, 90, 100, 125, 150, 175, 200, 250, 300, 350, 400, 450 and 500, so the volume varies from 1000 to 125000000 m^3, which represents the different volume of ordinary and large spaces) and 9 uniform absorption coefficients, from 0.1 to 0.9, were applied to all the surfaces in each space. The source points were arranged at the central point of the floor at a height of 1.5 m. Receiver height was 1.2 m. Fifteen points were arranged evenly in the quarter of floor in the smallest space because of the symmetry. And in the next larger space, 15 more points were arranged as the previous one. Receiver points in the previous space were also included in the next larger space for comparison.

3 Characteristics of sound field

Basic characteristics of sound energy distribution were explored in the measurements of four cases, as shown in Fig. 3. A near-exponential trend both appears in the distribution of total and reverberant energy in all four cases and this phenomenon is more obvious near the source. In the area far from the source, the attenuation gradually becomes linear. For each case, a polynomial regression is performed of the total sound level data as a function of source-receiver distance. The R^2 of regression in four cases varies from 0.87 to 0.92, which indicates that spatial difference between the points at the same source-receiver distance exists in a small range.

In order to further determine the spatial distribution of the reverberation energy in the space of larger volume and greater absorption coefficient, a series of cubes were simulated by an image-source method, the results of which are presented in Fig. 4. In the cubic space with a volume of 1000 m^3, the reverberant energy attenuates slightly with the increase of source-receiver distance. The difference range of reverberant energy in the space is 1.1 dB and 2.5 dB while the absorption coefficient is 0.3 and 0.7, respectively. This phenomenon is common in ordinary large spaces, such as auditoriums and small indoor stadiums. However, with the increase in volume and absorption coefficient, reverberant SPL shows a significant exponential decreasing trend. From Fig. 4, it is obvious that the curves become closer to the straight direct-energy line, since logarithmic abscissa axis is
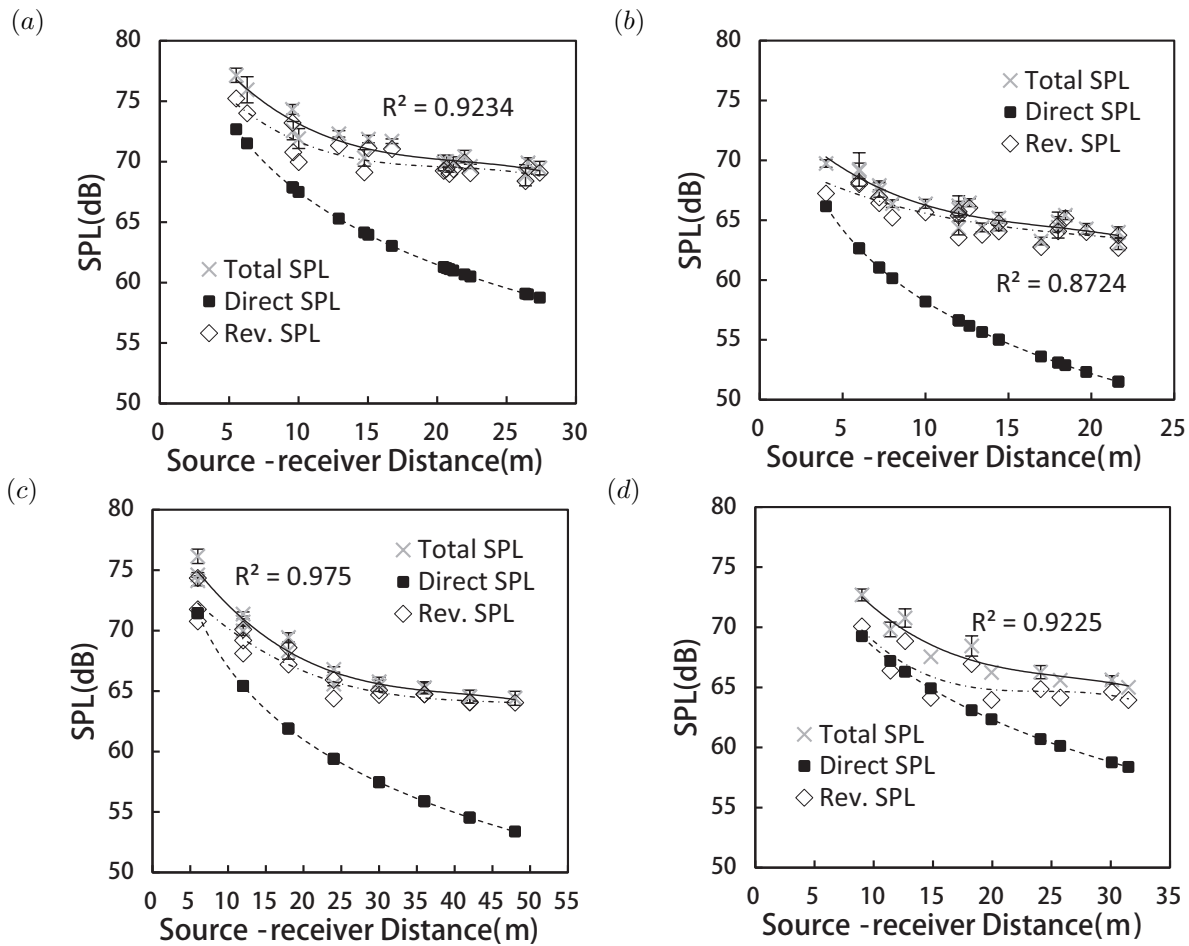
Figure 3: SPL distribution in four cases: (a) Dangxiao auditorium, (b) HIT indoor stadium, (c) TJU indoor stadium, and (d) Guian Circus Show. The curves of total SPL are obtained from the regression of measured points in different directions (represented by thick solid lines) and the regression coefficient is shown in each figure. The attenuation curves of the direct SPL (represented by dashed lines) could be derived from the source-receiver distance and the reverberant SPL (represented by dash-dotted lines) could be deduced from the energy relations in each case. The error bars represent the standard deviation of the three measured values of total SPL in the same receiver point.

used.

For large cubic spaces with side lengths of 100 m or more, the SPL profiles in Fig. 4 can be divided into three sections. The first part is the linear attenuate curve near the source and in different spaces those curves are always within about 6 m from the source. Then the second part shows an exponential trend in the remaining near-source area. More exponential trends appear with the increase of volume and the reverberant SPL curves of different spaces in the two figures move down and gradually approaches the first reflection from floor (FRFF) curve. The last part backs to the linear attenuate trend again in the area far from the source. This linear pattern is due to the domination of other reflections, which still have a slight attenuation with distance because the energy of FRFF decreases with the source-receiver distance. This three-part phenomenon in a large space is different from the hypothesis of classical model or other models [2, 22].

In terms of the effect of surface absorption, according to the relative relationship between the dash straight line and other curves in Fig. 4, the direct energy in the space with larger surface absorption occupies a greater proportion in total energy and shows more
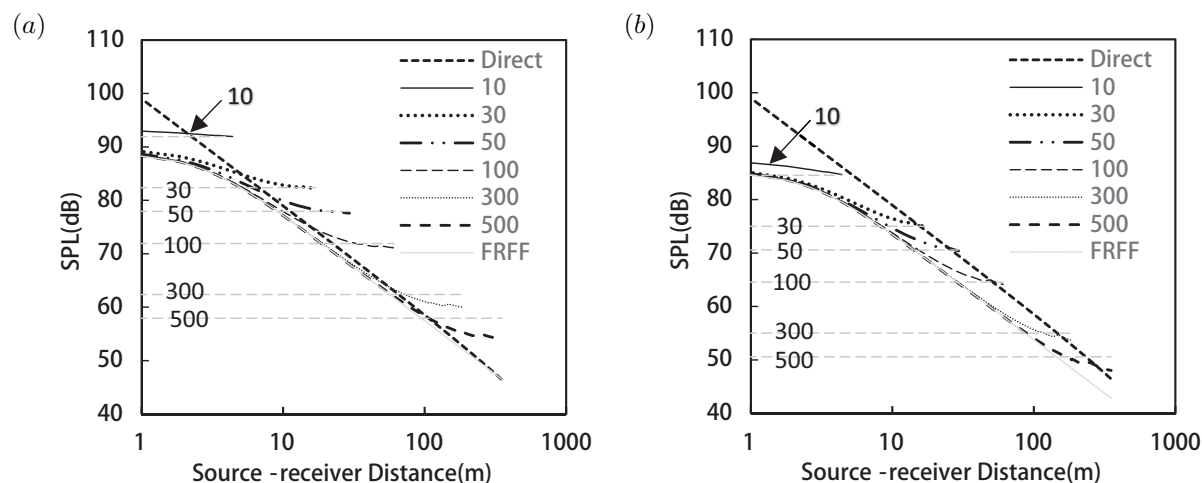
Figure 4: Theoretical reverberant SPL in cubic spaces of different volumes but with uniform absorption coefficients of (a) 0.3 and (b) 0.7. Parameter is side length in m, FRFF = first reflection from floor. Horizontal dashed lines represent the reverberant SPL according to classical theory.

exponential trends. Moreover, the curves in Fig. 4(a) are steeper than those in Fig. 4(b) which means that the reverberant energy also appears to be a more exponential trend with the growth of surface absorption. In each figure, this exponential trend is also more evident with the growth of volume. In this way, there is a larger distance range with exponential behaviour for larger room volumes and greater absorption coefficients.

4 Prediction model

The applicability of the classical model is first studied in this section. Then a new prediction model is proposed theoretically and validated with the measurements.

4.1 Applicability of classical model

The classical model [19] assumes that the reverberation sound energy is evenly distributed in a space, hence, the total SPL is

$$L = 10log_{10}(\frac{W}{4\pi r^2} + \frac{4W}{R}) + 120 \tag{1}$$

where W is the sound source power, r is the source-receiver distance, and R is the room constant.

As the volume becomes larger and the sound absorption coefficient increases, the spatial difference of reverberant energy increases correspondingly. Because it is difficult to determine the exact acoustic parameters in a real room, prediction results of the classical model are compared with those of computer simulation in the space of different volume and surface absorption.

The differences between prediction results of the total energy obtained by the classical model and the image-source method generally increase with the increase of volume and the decrease of surface absorption coefficient, as shown in Fig. 5. Air absorption here is neglected to highlight the effects of non-uniform early reflection energy and avoid differences of various considerations of air absorption. As can be seen in Fig. 4, the max difference between the reverberant energy derived from the classical model and the image-source

method always appears at the near-source area. Although the different range becomes larger with the increase of surface absorption, the reverberant-to-direct energy ratio is smaller simultaneously, which leads to the result that the total SPL difference is proportional to the size and inversely proportional to the surface absorption.
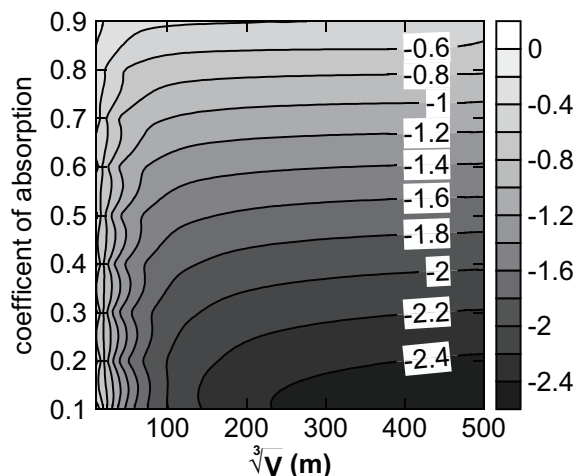

Figure 5: The prediction difference of the total energy (dB) obtained by the classical model and the image-source method (classical minus image-source method). Only the max absolute value of the difference was recorded in one space.

When the volume of a room is less than 8000 m^3 (of which the cube root is equal to 20 m), the difference between the classical model and image-source method is generally within 0.5 dB. The difference between the classical model and the image-source method is less than 1 dB when the absorption coefficient is less than 0.7 and the volume is less than 125000 m^3 (i.e. a 50 m cube). The difference is stationary below 1 dB when the absorption coefficient is larger than 0.7. Because this difference is due to the inhomogeneous spatial distribution of the reverberant energy, a curve in Fig. 5, say the 1 dB curve, might be used to distinguish ordinary large space and extra-large spaces.

4.2   A new prediction model

Different models to predict SPL distribution were proposed based on different considerations and approximations of reverberant energy. If the uniform decrease of reverberant energy with the increase of source-receiver distance was considered, a fixed rate factor was added by Barron [2] to predict the total SPL

$$L^B = 10log_{10}(\frac{W}{4\pi r^2} + \frac{4W}{R} \cdot e^{\frac{-13.82r}{cT_E}}) + 120 \tag{2}$$

where c is the velocity of sound, and T_E is the Eyring reverberation time. This model has good predictions in many concert halls.

Fig. 6 is helpful in explaining these models: t_c is the time at which the number of reflections is large enough to reach statistical average, which is also called averaging time [16]. Different statistical assumptions were made to predict the reflection energy before t_c. For example, the initial time t_0 and the time direct sound reaches t_D are used as the critical time in classical and Barron model respectively.
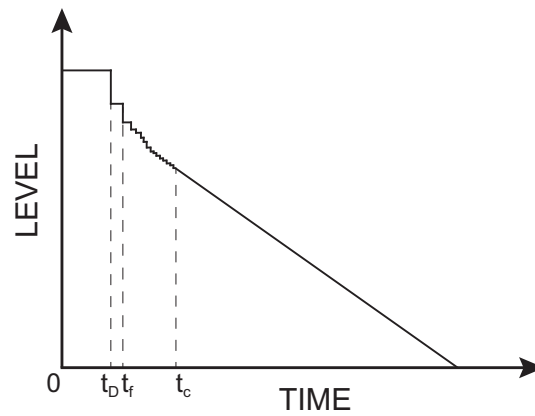
Figure 6:   Different stages of the energy decay.

Several other modified models were also proposed based on different approximations of early reflections [22, 23] and the rate of energy decay [24] but in some cases they did not show better accuracy[2].

However, the FRFF, which is significantly larger than the other reflections in general, has not been used to improve prediction accuracy. The path difference between the direct sound and the FRFF decrease with the source-receiver distance, as shown in Fig. 7, which results in a small difference in the energy in most areas. This is also consistent with the phenomenon in Fig. 4.
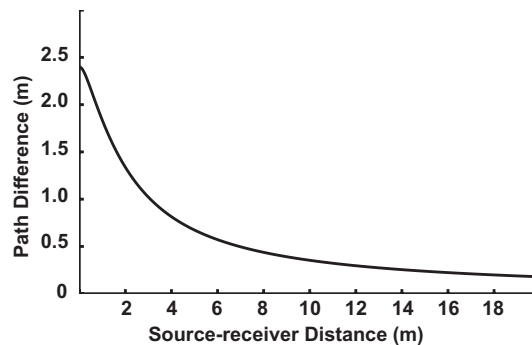

Figure 7:   Path difference between the direct sound and the first reflected sound from the floor.
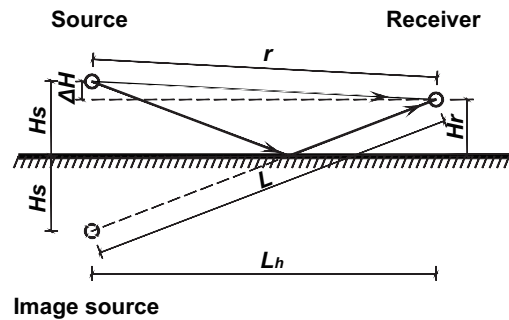

Figure 8:   The geometry of sound source and receiver points based on the image method.

In the current paper a newly modified model for extra-large spaces is therefore proposed based on the FRFF. The height of the source H_s and receiver H_r is 1.5 m and 1.2 m respectively, except where indicated. As both the source and receiver are closer to the floor than to the other surfaces in general, the reflection energy from the floor almost always reaches first in large spaces, which could be calculated as an individual term in a newly modified model. The time when the FRFF reaches t_f is considered a critical time for the statistical assumption in the new model. The reflection after t_f is still estimated by using the same statistical methods as in the Barron model which accuracy was confirmed by using the billiard theory [25] and measurements. Therefore, based on the geometry of sound source and receiver points, as shown in Fig. 8, the following three formulas can be obtained.

$$\Delta H = H_s - H_r \tag{3}$$

where ΔH is the height difference between the source and receiver points.

$$r^2 = (\Delta H)^2 + {L_h}^2 \tag{4}$$

where L_h is the horizontal distance between the source and receiver points.

$$L^2 = (2H_s - \Delta H)^2 + {L_h}^2 \tag{5}$$

where L is the path length of FRFF.

According to Eq. (3), Eq. (4) and Eq.(5), the path length of FRFF can be obtained by

$$L = \sqrt{4H_sH_r + r^2} \tag{6}$$

As the FRFF is considered, the total energy can be divided into three parts, which are the energy of direct sound, the FRFF and other subsequent reverberant sounds. So the total SPL can be obtained by

$$\begin{aligned} L' = \quad & 10log_{10}(\frac{W}{4\pi r^2} + \frac{W(1-\alpha_f)}{4\pi L^2} + \\ & \frac{4W}{R} \cdot e^{\frac{-13.82L}{cT}}) + 120 \end{aligned} \tag{7}$$

where α_f is the absorption coefficient of the floor; T is the reverberation time measured or calculated. Adding Eqs. (6) and (7), L' will be generated as:

$$\begin{aligned} L' = \quad & 10log_{10}(\frac{W}{4\pi r^2} + \frac{W(1-\alpha_f)}{4\pi(4H_sH_r + r^2)} + \\ & \frac{4W}{R} \cdot e^{\frac{-13.82\sqrt{4H_sH_r+r^2}}{cT}}) + 120 \end{aligned} \tag{8}$$

Theoretically, this model could not be used in the situation where the sound source, or the floor on which the first-order sound reflects, cannot be seen at the receiver point. The applicability in the situation where the source or receiver are far from the floor is also uncertain.

4.3   Validation of the new model

The modified model is applied to the four measured cases to obtain further validation, and the classical and Barron models are also used for comparison, as shown in Fig. 9. In the four cases, the absorption coefficient is calculated by the Eyring formula based on the reverberation time measured, and the sound power level of the source is deduced from the SPL measured at $1\ m$ from the source, since the direct energy here is about $9.5\ dB$ larger than the first reflect energy from the floor using the spherical formula.
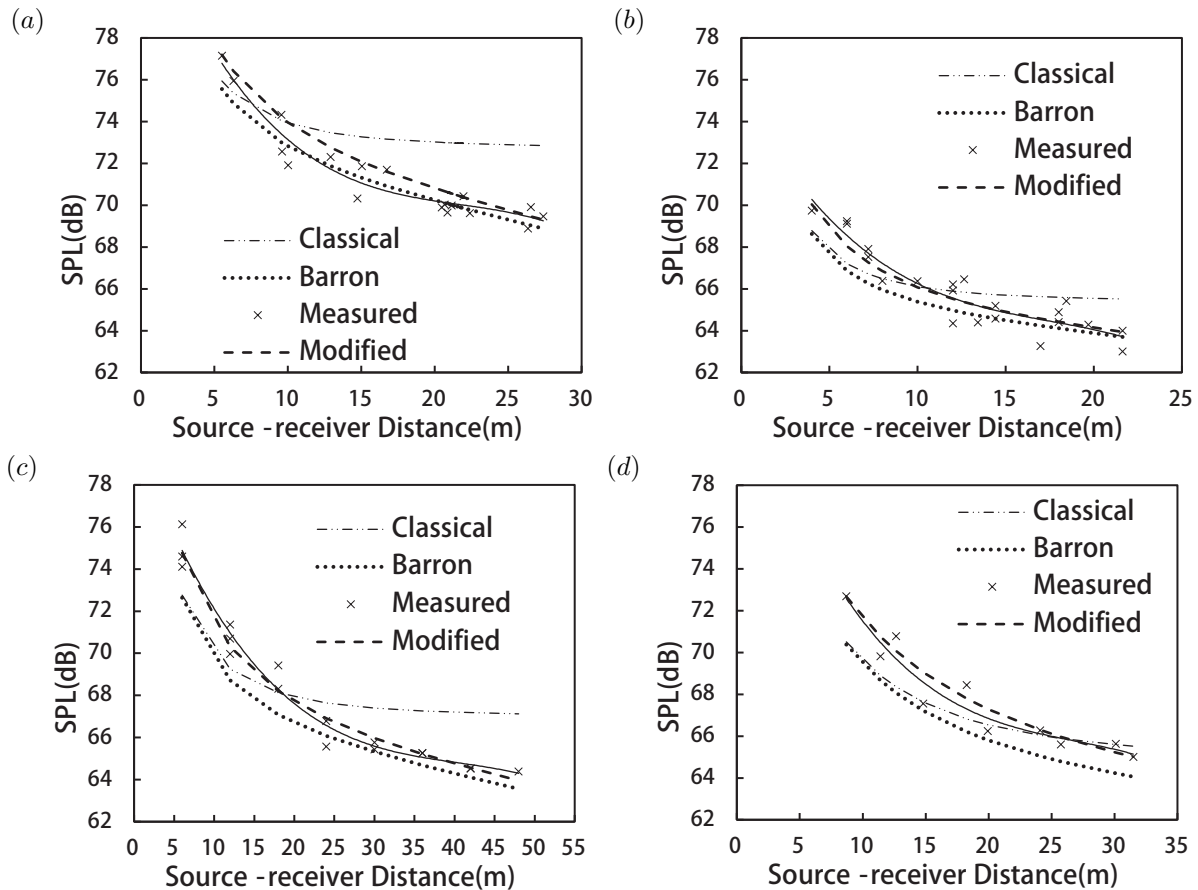

Figure 9:   Total SPL attenuation with the increase of source-receiver distance in measurement and prediction in four cases: (a) Dangxiao auditorium, (b) HIT indoor stadium, (c) TJU indoor stadium, and (d) Guian Circus Show.

As can be seen in Fig. 9, the results show that the classical model underestimated the energy in the near field, within about 10 to 20 m, and overestimated it in the far field. By adding a distance-dependent attenuation factor to reverberation energy, Barrons model yields very accurate predictions in the far field but still underestimated the energy in the near field. However, as the volume becomes larger and the first reflection energy from the floor has more advantages than other reflections, the accuracy is better using the modified model. The differences between the measurements and the modified model are significantly reduced. The maximum difference in the four cases is between 1.38 and 1.55 dB and the standard deviation is $0.66 - 0.71\ dB$, as shown in Table 2.

Further information is obtained from the simulation. The difference among the three models (classical, Barron, and the modified) and computer simulation shows different trends with the increase of the source-receiver distance, as shown in Fig. 10. When the

Table 2:   Differences of measured and predicted values by three models in four cases.

Cases	Classical			Barron			Revised		
	Min	Max	SD	Min	Max	SD	Min	Max	SD
Dangxiao auditorium	-1.7	3.49	1.46	-2.09	0.58	0.72	-0.94	1.55	0.66
HIT indoor stadium	-2.02	2.52	1.36	-2.36	0.98	0.9	-1.2	1.32	0.73
TJU indoor stadium	-3.38	2.72	1.95	-3.5	0.5	1	-1.38	1.33	0.66
Guian Circus Show	-2.4	0.52	1.03	-2.71	-0.34	0.77	-0.7	1.49	0.71

volume is 1000 m^3, all the three models have little differences, which are not larger than 1 dB. When the volume is 125000 m^3 and 125000000 m^3, both curves of the classical and Barron models show a deep trough at about $4 - 20$ m, which means a different degree of underestimation in the near-source area. This trough is mainly due to the FRFF and its relationship with other energy as in Fig. 4, it is proportional to the volume and inversely proportional to the absorption coefficient. When the surface coefficient is 0.1 and the volume is 125000000 m^3, the max difference between two existing models and computer simulation is 2.7 dB.

In Fig. 10, as the volume increases, the prediction difference of all the four models becomes greater generally and the difference curves show more spatial fluctuation with increasing source-receiver distance. This may suggest more theoretical limitations of statistical models in the extra-large spaces as the sound rays become more difficult to reach the statistical average with the increasing volume. Different from the two existing models, the prediction difference of the two modified models decreases with the increasing source-receiver distance. This is mainly due to the fact that the starting point of the calculation for the reverberant energy in the modified models is the latest among those models which results in less reverberant energy at the far-source point.

With regard to the use of Sabine or Eyring reverberation time, it is difficult to have the exact evidence to determine by computer simulation or measurements because most of the difference between the two formulas are within 1 dB as shown in Fig. 10, which still requires further study.

More details of the difference between the modified model and the image-source method are shown in Fig. 11. The modified model shows a better applicability in prediction and the accuracy of this new model is insensitive to volume, which shows more applicability in extra-large spaces. The max difference of total SPL appears when the surface absorption is 0.5.
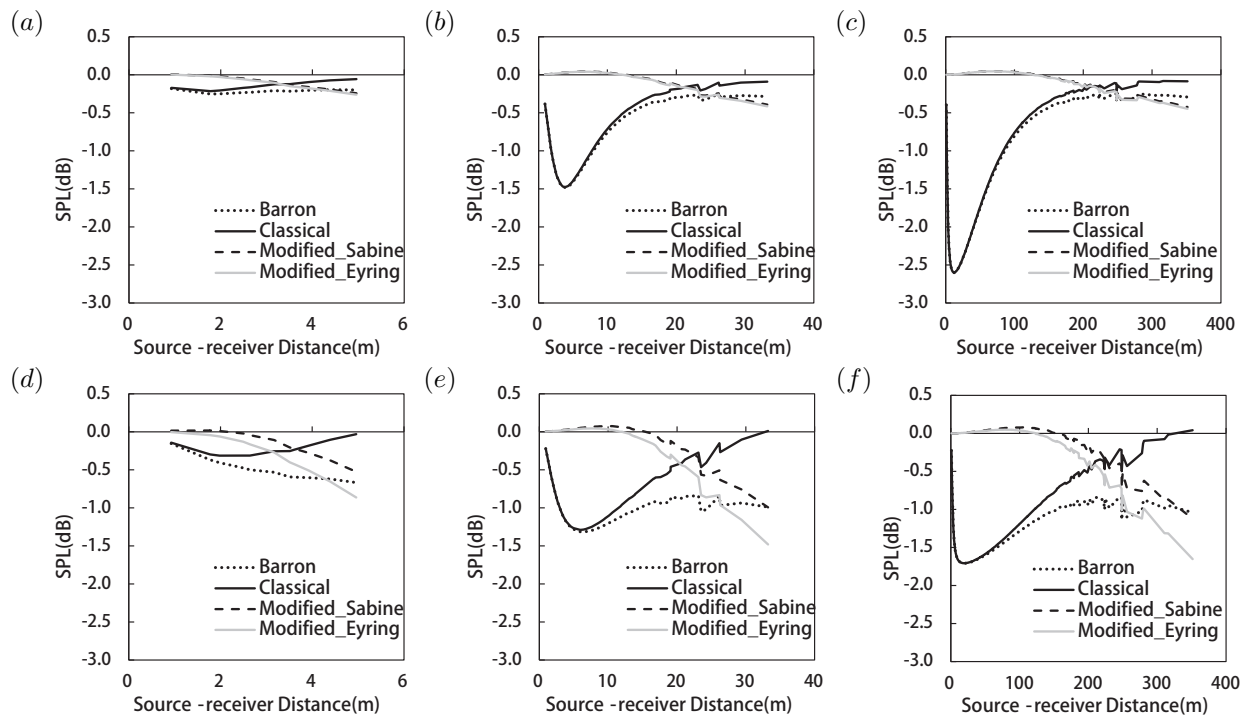
Figure 10: Difference in the results of models and computer simulation (models minus computer simulation). The dotted lines represent the Barron model, and the solid lines represent the classical model. The dashed and grey solid lines represented the modified model using Sabine and Eyring reverberation time respectively. (a), (b), and (c) were in the space with volumes 1000 m^3, 125000 m^3 and 125000000 m^3 respectively when the surface coefficient was 0.1. (d), (e), and (f) were in the space with volumes 1000 m^3, 125000 m^3 and 125000000 m^3 respectively when the surface coefficient was 0.5.
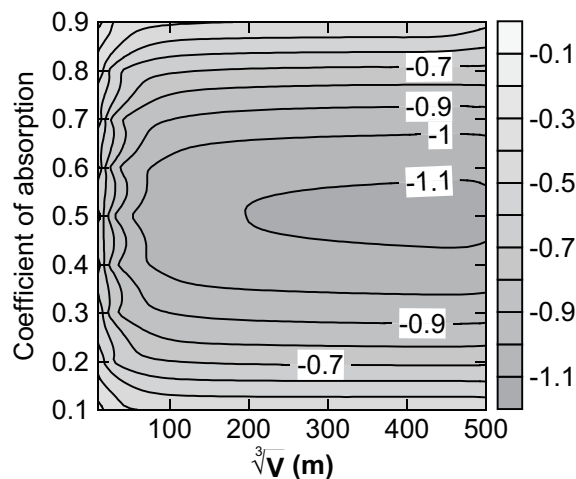

Figure 11: The prediction difference of the modified model and the image-source method (modified minus image-source method).

5 Conclusion

For SPL-prediction purposes, if 1 dB is accepted as the criterion, the space with the absorption coefficient is less than 0.7 and the volume is large than 125000 m^3 is suggested

to be called extra-large space based on the results of computer simulation in the current paper.

When a space volume becomes larger, the diffuse field assumption is more and more inapplicable not only for the total energy but also for the reverberant energy. The three-stage phenomenon was found in the attenuation of reverberant energy by using the image-source method and was validated in the following investigation. The first part is the linear attenuate curve near the source and then the second part shows an exponential trend in the remaining near-source area. The last part reverts to the linear attenuate trend again in the area far from the source. The importance of the first reflection from the floor in an extra-space is found to be the main reason of the three-stage attenuation.

A new model to predict the SPL attenuation in extra-large spaces is proposed based on the importance of the first reflection from the floor. In this model the energy of the first reflection from the floor can be calculated separately rather than being included in the approximate formula of the reverberant energy, and its accuracy and applicability were validated by two methods. In computer simulation, the advantage of the new model in the near-source area is indicated, and in four measured cases, the max difference is from 1.38 dB to 1.55 dB and the standard deviation of which is from 0.66 dB to 0.71 dB. This model could not be used in the situation where the sound source, or the floor on which the first-order sound reflects, cannot be seen at the receiver point. The applicability in the situation where the source or receiver is far from the floor is also uncertain.

6   Acknowledgements

References

[1] T. Fujikawa, S. Aoki, An escape guiding system utilizing the precedence effect for evacuation signal, in: Proceedings of Meetings on Acoustics, Vol. 19, Acoustical Society of America, 2013, p. 030055.

[2] M. Barron, Theory and measurement of early, late and total sound levels in rooms, The Journal of the Acoustical Society of America 137 (6) (2015) 3087–3098.

[3] M. Aretz, R. Orlowski, Sound strength and reverberation time in small concert halls, Applied Acoustics 70 (8) (2009) 1099–1110.

[4] J. Y. Jeon, Y. H. Kim, Design of sound diffusion in concert halls using scale models., The Journal of the Acoustical Society of America 127 (3) (2010) 1752–1752.

[5] Y. Soeta, K. Ito, R. Shimokura, S.-i. Sato, T. Ohsawa, Y. Ando, Effects of sound source location and direction on acoustic parameters in japanese churches, The Journal of the Acoustical Society of America 131 (2) (2012) 1206–1220.

[6] T. Zamarreño, S. Girón, M. Galindo, Acoustic energy relations in mudejar-gothic churches, The Journal of the Acoustical Society of America 121 (1) (2007) 234–250.

[7] T. Lewers, J. Anderson, Some acoustical properties of st paul's cathedral, london, Journal of Sound and Vibration 92 (2) (1984) 285–297.

[8] W. Joyce, Exact effect of surface roughness on the reverberation time of a uniformly absorbing spherical enclosure, The Journal of the Acoustical Society of America 64 (5) (1978) 1429–1436.

[9] R. Miles, Sound field in a rectangular enclosure with diffusely reflecting boundaries, Journal of Sound and Vibration 92 (2) (1984) 203–226.

[10] M. Hodgson, When is diffuse-field theory accurate?, Canadian Acoustics 22 (3) (1994) 41–42.

[11] A. G. Galaitsis, W. N. Patterson, Prediction of noise distribution in various enclosures from free-field measurements, The Journal of the Acoustical Society of America 60 (4) (1976) 848–856.

[12] H. Kuttruff, Stationary propagation of sound energy in flat enclosures with partially diffuse surface reflection, Acta Acustica united with Acustica 86 (6) (2000) 1028–1033.

[13] J. Kang, Acoustics in long enclosures with multiple sources, The Journal of the Acoustical Society of America 99 (2) (1996) 985–989.

[14] J. Picaut, L. Simon, J.-D. Polack, Sound field in long rooms with diffusely reflecting boundaries, Applied Acoustics 56 (4) (1999) 217–240.

[15] S. Tang, K. Piippo, Sound fields inside street canyons with inclined flanking building façades, in: Proceedings of Meetings on Acoustics 161ASA, Vol. 12, ASA, 2011, p. 040004.

[16] J. Anderson, M. Bratos-Anderson, Acoustic coupling effects in st paul's cathedral, london, Journal of sound and vibration 236 (2) (2000) 209–225.

[17] F. Martellotta, Identifying acoustical coupling by measurements and prediction-models for st. peters basilica in rome, The Journal of the Acoustical Society of America 126 (3) (2009) 1175–1186.

[18] J. J. Sendra, Computational acoustics in architecture, Wit Press, 1999.

[19] H. Kuttruff, Room acoustics, Crc Press, 2009.

[20] B. M. Gibbs, D. Jones, A simple image method for calculating the distribution of sound pressure levels within an enclosure, Acta Acustica united with Acustica 26 (1) (1972) 24–32.

[21] E. A. Lehmann, A. M. Johansson, Prediction of energy decay in room impulse responses simulated with an image-source model, The Journal of the Acoustical Society of America 124 (1) (2008) 269–277.

[22] E. Cirillo, F. Martellotta, Sound propagation and energy relations in churches, The Journal of the Acoustical Society of America 118 (1) (2005) 232–248.

[23] M. Vorländer, Revised relation between the sound power and the average sound pressure level in rooms and consequences for acoustic measurements, Acta Acustica united with Acustica 81 (4) (1995) 332–343.

[24] U. Berardi, E. Cirillo, F. Martellotta, A comparative analysis of acoustic energy models for churches, The Journal of the Acoustical Society of America 126 (4) (2009) 1838–1849.

[25] J.-D. Polack, Playing billiards in the concert hall: The mathematical foundations of geometrical room acoustics, Applied Acoustics 38 (2) (1993) 235–244.